30th Annual International IEEE EMBS Conference
Vancouver, British Columbia, Canada, August 20-24, 2008

Reservoir-wave separation and wave intensity analysis applied to carotid arteries: A hybrid 1D model to understand haemodynamics

Jazmin Aguado-Sierra, Justin E. Davies, Nearchos Hadjiloizou,
Darrel Francis, Jamil Mayet, Alun D. Hughes and Kim H. Parker

Abstract— **Pressure waveforms measured at different locations in the cardiovascular system present a very similar diastolic decay. Previous work has shown the cardiovascular system can be modelled as a Windkessel and wave system. This concept has been extended to any arbitrary location in the cardiovascular system.**

We suggest that it is possible to calculate a time-varying reservoir pressure $\bar{P}(t)$ and a distance- and time-varying wave pressure $p(x,t)$ by fitting an exponential function to the diastolic decay of the measured pressure P; defining that the measured pressure $P(x,t) = \bar{P}(t) + p(x,t)$. Velocity waveforms U can also be separated into its reservoir, $\bar{U}$, and wave, u, components as $U(x,t) = \bar{U}(x,t) + u(x,t)$.

In this study we explore the implications of applying a reservoir-wave separation and wave intensity analysis techniques to understand the haemodynamics of *in-vivo*, non-invasive measurements of P and U in the carotid arteries of normal human subjects. Wave intensity analysis reveals a particular wave pattern where reflections can be estimated easily, but foremost, it shows that reflections are a lot smaller than previously thought.

We suggest through the use of this model that the heart is the main wave generator of the cardiovascular system. The arterial system instead of impeding the flow, it stores it and distributes it throughout the arteries towards the tissue during diastole. There are some wave reflections, mainly during systole, that contribute to the changes in the pressure and velocity waveforms, however, they are small and are more evident as the measurements get further away from the ascending aorta.

The application of wave intensity analysis to non-invasively measured data can provide a good insight on the physiology and the local and global properties of the cardiovascular system in health and disease in the clinical setting. This study shows preliminary results and the potential of the technique for analysing non-invasive measures, and could be particularly useful to understand and quantify the effects of therapeutic drugs in the cardiovascular system.

I. INTRODUCTION

The Windkessel model highlights the importance of the arterial compliance in transforming the discontinuous cardiac output into a more steady pressure and flow in the periphery. This model excels in explaining the diastolic part of the pressure waveform, but it fails to reproduce the systolic part because pressure changes are assumed to occur simultaneously throughout the arteries without accounting for the wave nature of pulse wave propagation. [4]

Previous studies [1] model the flow in the aorta as a time domain Windkessel and wave system that relies upon measurement of pressure and velocity in the ascending aorta. We extended this concept [2], [3] to any arbitrary location in the cardiovascular system based on empirical hypotheses. It is also suggested that both pressure ($P(t)$) and velocity ($U(t)$) in the systemic arteries can be decomposed into a reservoir and wave components, and that they are directly related.

Wave intensity analysis provides information about the net wave interaction in the arterial system. It employs infinitesimal changes in pressure and velocity $(dP/dt) \cdot (dU/dt)$. [5] This technique has been widely employed to understand the haemodynamics of normal and pathophysiological states in the experimental and clinical setting. We now suggest that the reservoir-wave components of the pressure and velocity have to be taken into account when wave intensity is used. Furthermore, it is necessary to extract the reservoir components from the calculations to be able to distinguish forward waves from reflected ones. By doing so, it is clearly noticeable that reflection waves are smaller than previously thought. These small reflected waves give clear information on the nature of bifurcations in the arterial system. The arterial system is generally a well matched system. Large reflected waves are unable to travel and be seen at the ascending aorta, for example, which agrees with the literature regarding wave reflection experiments [6], [7], [8]. The reflected waves increase in size with the increase in distance from the aortic valve; however, they remain relatively small in comparison to the forward waves propagating from the heart. It has been observed that the greatest wave generator in the cardiovascular system is the heart and it relies on the arterial system to sustain its function and physiology [2].

II. METHODS

A. Experimental Methods

Non-invasive measurements of pressure, velocity and diameter in left and right carotid arteries were obtained from subjects with no stenosis and no haemodynamically significant atheroma (8 males; aged 23 - 31 years). All in-vivo studies were approved by the St. Mary's Hospital local ethics committee and performed in accordance with institutional guidelines; all participants provided full informed consent. The R wave of the ECG was used as a fiducial marker. Flow velocity was measured using an ultrasound machine Aloka 5500SV (Aloka Inc, Tokyo, Japan.) It also provides an in-built wave intensity analysis system and uses an e-tracking technique (see Fig. 1) from which a pressure waveform is obtained assuming that changes in diameter are linearly

Dr. Aguado-Sierra was supported by CONACyT
This study was performed as part of the Physiological Flow Studies Group, Bioengineering Department, at the ICCH, St. Mary's Hospital, Imperial College London, London, UK
jazmin.aguado03@imperial.ac.uk

related to changes in pressure [9]. Pressure was also measured using an Arterial Applanation Tonometer. Each signal measured is digitised, using a NiDAQ acquisition board. Brachial blood pressure was measured using an automated device Omron HEM-705-CP (Omron Corp, Kyoto, Japan). The mean pressure is considered equal to the mean carotid pressure. [10]

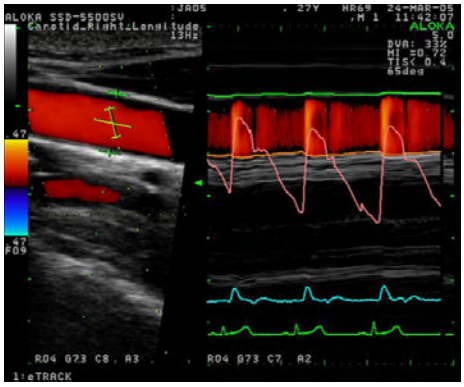

Fig. 1. P and U measured in the right carotid artery of a normal human subject. All the data shown corresponds to the same subject.

B. Theoretical Methods

The empirical algorithm to extend the theory proposed by [1] was programmed using Matlab (The MathWorks, Massachusetts, USA) and it is based on the following observations:

1) The pressure waveform decay measured at different locations in the arterial system is very similar in diastole. For example, the pressure measured in the carotid arteries is very similar to the pressure waveform measured in the ascending aorta, although the flow waveforms are qualitatively different.
2) When the wave pressure in the ascending aorta (the difference between the measured pressure and the reservoir pressure calculated from the measured flow) is plotted against the measured flow waveform, an almost straight line is obtained. [1] This indicates that the flow in the ascending aorta is dominated by forward waves, which indicates that arterial bifurcations are close to well-matched for forward waves and, hence, the wave pressure measured at any aortic location is approximately proportional to the cardiac output. Observation of well-matched bifurcations for forward waves in humans has been reported. [11]

Under these assumptions, it is possible to determine a reservoir pressure, $\bar{P}(t)$, from a pressure waveform, $P(x,t)$, measured at an arbitrary location in the arterial tree. Assuming that $\bar{P}(t)$ is determined from the conservation of mass, as previously described by [3],

$$\frac{\mathrm{d}\bar{P}(t)}{\mathrm{d}t} + \frac{\bar{P}(t) - P_v}{RC} = \frac{Q_{in}(t)}{C}. \tag{1}$$

Where P_v is the venous pressure or tissue pressure; R is the resistance and C is the capacitance determining the reservoir effect. By the second observation (assumption), we can approximate $Q_{in}(t) = \gamma(P(t) - \bar{P}(t))$, where γ is a constant which will depend upon a number of factors, such as the local wave speed and cross-sectional area. Therefore, (1) leads to

$$\frac{d\bar{P}}{dt} = a(P(t) - \bar{P}(t)) - b(\bar{P}(t) - P_v), \tag{2}$$

where $a = \gamma/C$ and $b = 1/RC = 1/\tau$ are rate constants of the system with units s^{-1}.

Under normal conditions, $Q_{in}(t) = 0$ for $T_N \leq t \leq T$, where T_N is the time when the aortic valve shuts at the end of systole and T is the time when the heart beat ends. During this period of time (2) reduces to

$$\frac{d\bar{P}}{dt} = -b(\bar{P}(t) - P_v), \qquad T_N \leq t \leq T. \tag{3}$$

T_N corresponds to the time when the dicrotic notch appears in P. In case of a pressure waveform without a clearly marked notch, T_N is taken to be the time of the first zero-crossing of the second derivative of pressure at the end of systole. The solution of (3) is

$$\bar{P}(t) - P_v = (\bar{P}(T_N) - P_v)e^{-b(t-T_N)}, \qquad T_N \leq t \leq T. \tag{4}$$

Considering that the reservoir effect is the main driver of the exponential pressure fall off in diastole, and waves are minimal, the constant parameters $\bar{P}(T_N)$, P_v and b can be estimated by fitting them to experimental data P using (4).

For systole, (2) can be solved explicitly as

$$\begin{aligned}\bar{P}(t) = \frac{b}{a+b}P_v + e^{-(a+b)t}\left[\int_0^t aP(t')e^{(a+b)t'}dt'\right] \\ + e^{-(a+b)t}\left[\bar{P}_{(t=0)} - \frac{b}{a+b}P_v\right],\end{aligned} \tag{5}$$

where $\bar{P}_{(t=0)}$ corresponds to the start point of the onset of P, since little wave activity is expected at the end of the previous beat. Note that the second observation needs only to be true during the systolic period, $0 \leq t \leq T_N$. To determine the unknown parameter a we enforce continuity of $\bar{P}$ at $t = T_N$, which yields

$$\begin{aligned}\bar{P}(T_N) = \frac{b}{a+b}P_v + e^{-(a+b)T_N}\left[\int_0^{T_N} aP(t')e^{(a+b)t'}dt'\right] \\ + e^{-(a+b)T_N}\left[\bar{P}_{(t=0)} - \frac{b}{a+b}P_v\right].\end{aligned} \tag{6}$$

The parameter a is fitted from experimental data using an unconstrained nonlinear optimisation routine. Then $\bar{P}$ is determined for the entire period from (4) and (5).

Note that data were non-dimensionalised. The Matlab routine *fminsearch* was used to estimate $\bar{P}(T_N)$, b and a with non-dimensionalised initial conditions equivalent to $\bar{P}(T_N) = P(T_N)$, $b = 1\ \mathrm{s}^{-1}$ and $a = 10\ \mathrm{s}^{-1}$, respectively, and a tolerance of $1e^{-12}$. P_v was fixed to $P_v = 25\mathrm{mmHg}$ (3.333kPa). [14]

1) Reservoir velocity: The velocity due to the reservoir pressure, $\bar{U}$, is assumed to be zero in the model by [1]. This is a good assumption in the ascending aorta. However, it should not be true in more distal vessels. Therefore both the pressure and the velocity can be resolved into a reservoir and a wave component; $U(x,t) = \bar{U}(x,t) + u(x,t)$.

$\bar{U}(x,t)$ is directly proportional to $(P(t) - P_v)$ during diastole when there is little wave activity,

$$\bar{U}(x,t) = \bar{R}(P(t) - P_v), \tag{7}$$

where $\bar{R}$ is the effective resistance of the vessels downstream of the measurement site. There is a linear relationship of slope $\bar{R}$ between $P(t)$ and $U(t)$ at the end of diastole when wave activity is minimal.

$\bar{R}$ is determined as $\bar{R} = (< P(t) > - P_v) / < U(t) >$, where $< P(t) >$ and $< U(t) >$ are the time-averaged pressure and velocity for $T_N \leq t \leq T$.

We can then calculate $\bar{U}(t)$ at any time $0 \leq t \leq T$ as

$$\bar{U}(x,t) = \bar{R}(\bar{P}(t) - P_v). \tag{8}$$

The wave velocity is then $u(x,t) = U(t) - \bar{U}(x,t)$, which will generally be non-zero except at the root of the aorta during diastole.

III. Results

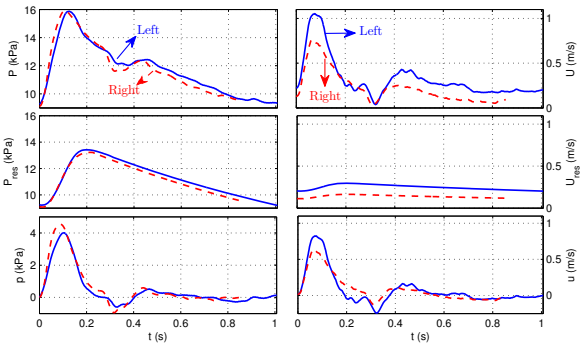

Fig. 2. Reservoir-wave components of measured P and U at left (blue solid line) and right (red dashed line) carotid arteries of the same subject. Left panels show P components; right panels show U components. At top, measured waveforms; Middle, reservoir components. At bottom, wave components.

Carotid Artery	τ (s)	$\bar{R}$ (kPa·s/m)	constant fitted in systole, a (s^{-1})	D_s (mm)	D_d (mm)
Left	1.44	45.4	10.93	6.32	5.36
Right	1.35	80.6	9.43	7.92	7.15

TABLE I

TIME CONSTANT VALUES OF THE DIASTOLIC DECAY τ (S) IN THE LEFT AND RIGHT CAROTID ARTERIES; THE AVERAGE DIASTOLIC RESISTANCE ($\bar{R}$) CALCULATED FROM SIMULTANEOUS *in-vivo* P AND U MEASUREMENTS; THE FITTED CONSTANT IN SYSTOLE, a; DIAMETER AT SYSTOLE, D_s; AND DIAMETER AT DIASTOLE, D_d.

It is possible to interpret the measured arterial pressure and velocity in the carotid arteries as the sum of a reservoir and wave components. Figure (2) shows the results from applying the separation method to both P and U waveforms from left and right carotids. Notice that it holds in the carotid arteries that the reservoir components $\bar{P}$ and $\bar{U}$ are very similar in both vessels, as can also be observed from the values of τ in Table I. It also holds true that the wave components p and u are strongly related, and they only vary when reflected waves exist. Table I shows the parameters obtained from the fit and the systolic, D_s, and diastolic, D_d, diameters for each vessel.

Wave speed, c, was also calculated using the sum of the squares ($c_{\sum^2}$) technique [12] using only the wave components p and u (see Table II). Wave speed was also calculated using the PU-loop (c_{PU}) [8] and pu-loop (c_{pu}). It is noticeable that if we only employ the wave components for calculating wave speed, we still obtain a good estimate, as can be observed in Fig. (3). Wave p and u retain the information of wave propagation.

Carotid	$c_{\sum^2}$ (m/s)	c_{PU} (m/s)	c_{pu} (m/s)
Left	3.9	4.0	3.5
Right	7.0	7.8	6.7

TABLE II

WAVE SPEED VALUES $c_{\sum^2}$ c_{PU} AND c_{pu} ESTIMATED IN THE LEFT AND RIGHT CAROTID FROM P AND U NON-INVASIVE MEASURED DATA.

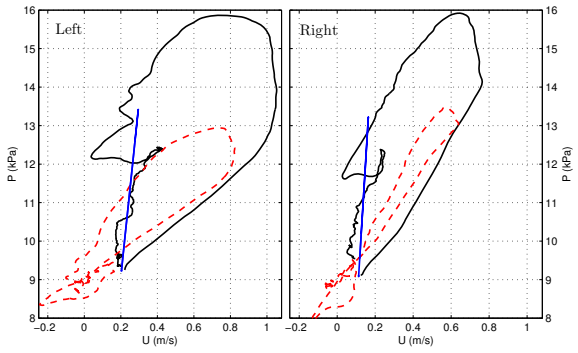

Fig. 3. Left and right carotid PU-loops (black, solid line), $\bar{PU}$-loop (solid, blue line) and pu-loop (red, dotted line).

When we calculate the wave intensity (see Fig. 4) the reservoir component accounts for very little or no wave activity; therefore, it only reduces the magnitude of the wave intensity by less than 20%. This is due to the slow changes in time of the reservoir behaviour in normal conditions. Wave intensity analysis is used to separate forward and backward waves; for which we used $c_{\sum^2}$. Figure (4) shows in the top panels, the net wave intensity. Notice that reflected or backward waves are small (see Fig. 4, mid and lower panels, dotted lines). Waves travel mostly forward from the heart; a large forward compression wave (in blue) initially drives the flow at the beginning of systole. A forward expansion wave stops the blood flow. This wave could be the result of the slowing down of the myocardium, and some reflected waves,

seen as forward travelling in the carotids. We can see small backward travelling, reflected waves (yellow and red), which indicate that the main site of reflection is located at 6.6 cm distance from the measurement site in the left carotid; and for the right carotid, the main reflection site can be located at 17 cm.

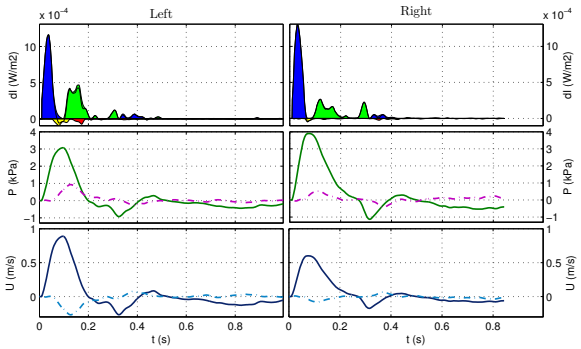

Fig. 4. Wave intensity analysis in left and right carotids is shown in top panels. Forward compression waves, or forward accelerating waves in blue; backward expansion waves, or backward accelerating waves in red; forward expansion waves, or forward decelerating waves in green; backward compression waves, or backward decelerating waves in yellow. Wave separation of P (in mid panels) and U (in lower panels). Forward travelling waves in solid lines; and backward travelling waves or reflected waves, in dotted lines.

IV. CONCLUSIONS

Non-invasive measurements in the carotid arteries of human patients are easily obtained in the clinical setting. A reservoir plus a wave pressure may be a useful model for obtaining local and global information of the cardiovascular system from non-invasive measurements. Wave intensity analysis can provide a different interpretation of wave travel when the reservoir component is extracted from the data. We suggest through the use of this model that the heart is the main wave generator of the cardiovascular system. The arterial system instead of impeding the flow, it stores it and distributes it throughout the arteries towards the tissue during diastole. There are some wave reflections, mainly during systole, that contribute to the changes in the pressure and velocity waveforms, however, they are small and are more evident as the measurements get further away from the ascending aorta. The reservoir behaviour is a global parameter of the cardiovascular system that can provide useful information, particularly as it can be obtained non-invasively in the clinical setting.

REFERENCES

[1] Wang, J-J., O'Brien, A.B., Shrive, N.G., Parker, K.H. and Tyberg, J.V., Time-domain representation of ventricular-arterial coupling as an windkessel and wave system, *Am J Physiol Heart Circ Physiol*, vol. 284, 2003, pp 1358-1368.

[2] Aguado-Sierra J., Alastruey J., Wang J-J., Hadjiloizou N., Davies J.E., Parker K.H., Separation of the reservoir and wave pressure and velocity from measurements at an arbitrary location in arteries. Proceedings of the Institution of Mechanical Engineers, Part H, Journal of Engineering in Medicine. Accepted Nov 2007.

[3] Aguado-Sierra, J., Hadjiloizou, N., Davies, J.E., Francis, D.P., Mayet, J., Parker, K.H., Pressure reservoir-wave separation applied to the coronary arterial data, *Proceeding of the Engineering in Medicine and Biology Society, Lyon, France*, 2007, pp. 2693-2696.

[4] Frank, Otto., Die Grundform des Arteriellen Pulses, *Z. Biol.*, 1899, vol. 37, pp. 483-526.

[5] Parker, K.H. and Jones, C.J.H., Forward and backward running waves in the arteries: analysis using the method of characteristics, *J. Biomech. Eng.*, 1990, vol. 11, pp. 322-326.

[6] Peterson, LH., The dynamics of pulsatile blood flow, *Circulation Research*, 1954, vol. 2, pp. 127-139.

[7] Nichols, WW. and O'Rourke, MF., *McDonald's Blood Flow in Arteries. Theoretical, experimental and clinical principles*, Ed. Edward Arnold, Fifth Edition, London, 2005.

[8] Khir, AW. and Parker, KH., Measurements of wave speed and reflected waves in elastic tubes and bifurcations, *Journal of Biomechanics*, 2001, vol. 35, pp. 775-783.

[9] Sugawara, M., Niki, K., Furuhata, H., Ohnishi, S., Suzuki, S., Relationship between the pressure and diameter of the carotid artery in humans, *Heart Vessels*, 2000, vol. 15, pp 49-51.

[10] Van Bortel, LM., Balkestein, EJ., Heijden-Spek, J.J. vd, Vanmolkot, F.H., Staessen, J.A., Kragten, J.A., Vredeveld, J.W., Safar, M.E., Struijker Boudier, H.A., Hoeks, A.P., Non-invasive assessment of local arterial pulse pressure: comparison of applanation tonometry and echo-tracking, *Journal of Hypertension*, 2001, vol. 19,(6), pp. 1037-1044.

[11] Papageorgiou, GL., Jones, NB., Arterial system configuration and wave reflection, *Journal of Biomedical Engineering*, 1987, vol. 9, pp. 299-301.

[12] Aguado-Sierra, J., Parker, Kim H., Davies, J.E., Francis, D.P., Hughes, A.D., and Mayet, J., "Arterial pulse wave velocity in coronary arteries", *Proceedings of 28th Annual International Conference of the IEEE EMBC*, New York, New York, USA, August 2006.

[13] Justin E. Davies, Zachary I. Whinnett, Darrel P. Francis, Charlotte H. Manisty, Jazmin Aguado-Sierra, Keith Willson, Rodney A. Foale, Iqbal S. Malik, Alun D. Hughes, Kim H. Parker and Jamil Mayet, Evidence of a dominant backward-propagating "suction" wave, responsible for diastolic coronary filling in humans, attenuated in left ventricular hypertrophy, *Circulation*, vol. 113, 2006, pp. 1768-1778.

[14] Schipke, J.D., Heusch, G., Sanii, A.P., Gams, E., and Winter, J., Static filling pressure in patients during induced ventricular fibrillation, *Am J Physiol Heart Circ Physiol*, 2003, vol. 285, pp. 2510-2515.